procedure is followed with the initial assumption that all of the scattering is first order, the resultant functions B and G may be used to compute from equation (9) I_{TD2}. This may then be subtracted from the measurements to obtain better values of the first order diffuse intensity. Iteration of this procedure may be followed to self-consistency, yielding values of first and second order temperature diffuse scattering to any precision desired. Expressions similar to, but more involved than, equation (9) may clearly be developed to obtain expressions for higher order diffuse components of the diffraction pattern if that is necessary. Though the day is not long past when the computation involved in equation (9) would have appeared formidable, the above described iteration procedure may be carried out very easily with a modern computer.

If the usual harmonic representation of the atomic displacements in terms of superposed waves is incorporated into equations (2) and (7), they become James's (1965) equation (5·45) for I_{TD1} and Walker's (1953) equation (4) for I_{TD2}. However, though the harmonic model is used, the usual normal mode representation of the diffuse intensity is not. Since the result for I_{TD1}

is not dependent on the harmonic approximation, this representation of first order intensity in terms of the mean atomic displacements is valid even if there are large anharmonic contributions so that the usual theory does not apply. Without the harmonic approximation the simple representation of I_{TD2} in terms of the functions B and G given by equation (9) no longer holds. Even in that case the above described method for correction for I_{TD2} may still be an acceptable approximation.

References

BORIE, B. (1961). Acta Cryst. 14, 566.
BORIE, B. & SPARKS, C. J. (1965). Metals and Ceramics Div. Ann. Progr. Rept. 30 June 1965, ORNL-3870, p. 80. Oak Ridge National Laboratory, Tennessee.
JACOBSEN, E. H. (1955). Phys. Rev. 97, 654.
JAMES, R. W. (1965). The Optical Principles of the Diffraction of X-rays. London: Bell.
JOYNSON, R. E. (1954). Phys. Rev. 94, 851.
OLMER, P. (1948). Bull. Soc. franç. Minér. 71, 145.
PASKIN, A. (1958). Acta Cryst. 11, 165.
PASKIN, A. (1959). Acta Cryst. 12, 290.
WALKER, C. B. (1953). Acta Cryst. 6, 803.

Monoclinic–Tetragonal Phase Transition in Zirconia: Mechanism, Pretransformation and Coexistence

BY R. N. PATIL AND E. C. SUBBARAO

Indian Institute of Technology, Kanpur, U.P., India

The high temperature X-ray diffraction study of the monoclinic–tetragonal phase transition in ZrO_2 showed that it is spread over a temperature range 930–1220°C. Anomalous intensity changes are observed in the pretransformation region 930–1100°C. Coexistence of phases through hybrid crystal formation in the region 1100–1220°C and the mechanism of transition are discussed. The orientation relationship between the monoclinic (m) and the tetragonal (t) crystal structures consists in the parallelism of the $(100)_m$ plane to $(110)_t$ and of the b_m axis to the c_t axis. A drastic change in a small temperature range during the tetragonal–monoclinic transition is interpreted as a cooperative change in both short and long range interactions. The large thermal hysteresis is attributed to the difference in the mechanism of transition during heating and cooling.

Introduction

The monoclinic–tetragonal transition in ZrO_2 has been extensively investigated (Baun, 1963; Cypres, Wollast & Raueq, 1963; Grain & Garvie, 1965; Hinz & Dietzel, 1962; Sukharevskii, Alapin & Gavrish, 1964; Whitney, 1962; Wolten, 1963, 1964) using differential thermal analysis, dilatometry, high pressure studies and X-ray diffractometry. Considerable disagreement among different investigators prevails regarding the transformation temperature and thermal hysteresis. The disagreement may be due to: (i) the dynamic study of the transition and (ii) the type of impurities present.

Wolten (1963, 1964) described the monoclinic–tetragonal transformation in ZrO_2 to be diffusionless and likened it to the martensitic type of transformation observed in metallic and alloy systems. Athermal kinetics, thermal hysteresis and the shearing mechanism due to the atomic displacements during the transformation are characteristics of the martensitic type of transformation. The electron microscopic studies of Bailey (1964) and metallographic observations by Fehrenbacher & Jacobson (1965) support Wolten's work and attribute a shearing mechanism to the atomic movements during the phase change. Sukharevskii et al. (1964) associate an isothermal component in the

transformation with the defects in the structure. Grain & Garvie (1965) report the effect of grain size on the kinetics and the heat of transition; they describe it as a continuous transformation according to Ubbelohde's (1956) classification scheme. In a recent study Gavrish & Krivoruchko (1966) report the effect of heating rate and impurities on the transition temperature and establish a relation to describe the kinetics of the transition. Based on an assumption that the transformation proceeds by nucleus growth of a new phase, they go on to calculate the interfacial tension coefficient. So far, the mechanism of the monoclinic–tetragonal transition in ZrO_2 has not clearly been established.

The present investigation aims at a study of the monoclinic–tetragonal transition in ZrO_2 by high temperature X-ray diffraction at a number of test temperatures maintained for sufficient time in the coexistence region. A careful study of the positions and the intensities of the X-ray diffraction maxima in the coexistence region was made, to elucidate the mechanism of the transition during heating and cooling in terms of the possible atomic movements and the sequence of changes. The movements of the oxygen atoms during transition, inferred from the present study, confirmed the intuitive suggestions made by Smith & Newkirk (1965). Their suggestions were based on the comparison of the two crystal structures, monoclinic and tetragonal.

Experimental

The ZrO_2 used in this study was obtained from the Atomic Energy Establishment, Trombay, India and has Hf (0·02%) and Si (0·1%) as major impurities. The X-ray diffraction work was carried out on a General Electric XRD-6 diffractometer with a Tem-Pres Research high temperature furnace. Filtered Cu $K\alpha$ radiation was used. The experimental set-up used for the study of the monoclinic–tetragonal transition in ZrO_2 at different test temperatures in the coexistence region of the transition during heating as well as during cooling was the same as that employed for the determination of axial thermal expansion of ZrO_2 (Patil & Subbarao, 1969). The desired temperatures were maintained within $\pm4°C$ with the help of a Pt/Pt–10% Rh thermocouple and a commercial controller. The temperatures were maintained for 5 to 10 minutes before

recording at any test temperature in order to allow the specimen to attain thermal equilibrium. Time-dependent behaviour in the transition region was not studied. The reflexions followed in the study were $11\bar{1}_m$, 111_m, 002_m, 020_m, 200_m, 101_t, 002_t, 110_t indexed on the primitive structures given by McCullough & Trueblood (1959), and Teufer (1962). The suffixes m and t refer respectively to the monoclinic and the tetragonal phases.
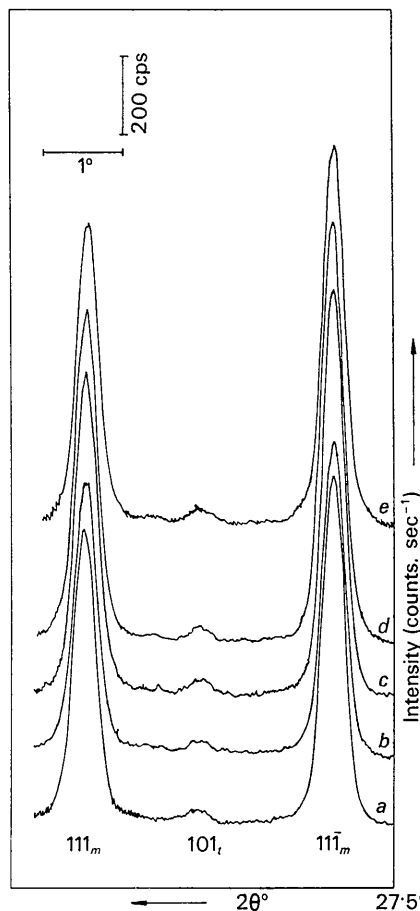

Fig. 1. Reflexions corresponding to $(11\bar{1})_m$, $(101)_t$ and $(111)_m$ in the pretransformation region of monoclinic–tetragonal phase transition in ZrO_2 on heating. Records a, b, c, d and e refer to temperatures, 892 932, 978, 1023 and 1048°C respectively.

Table 1. *Intensities of* $11\bar{1}_m$, 111_m *reflexions in the pretransformation region during heating*

Arbitrary units – intensities of the reflexions at room temperature are taken as 100. A specimen was heated, cooled, and reheated to obtain the two sets of data during heating.

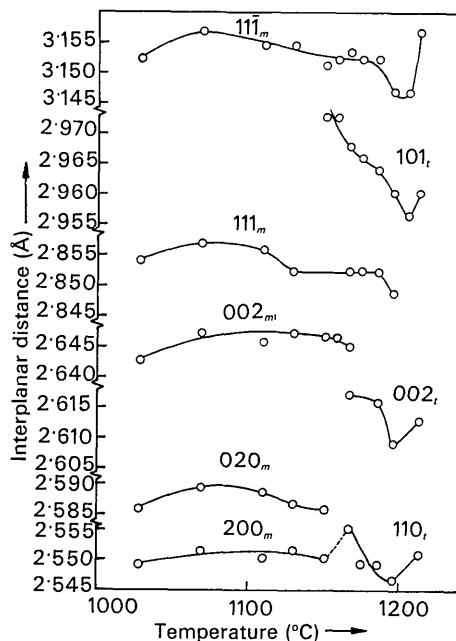| First run			Second run		
Temperature	$11\bar{1}_m$	111_m	Temperature	$11\bar{1}_m$	111_m
892°C	89	97	798°C	89	92
932	83	95	932	104	119
978	102	112	956	111	114
1023	107	110	985	115	121
1048	97	101	1014	112	116
			1040	117	121

Fig. 2. Temperature dependence of the interplanar distances in the monoclinic–tetragonal transition region.

Results and discussion

The monoclinic–tetragonal transition in ZrO_2 is spread over the temperature range 930–1220 °C during heating and 1030–700 °C during cooling. Since the mechanism of phase transition during heating appears to be different from that during cooling, the two are treated seperately.

Monoclinic–tetragonal transition

Two distinct temperature ranges may be identified in the transition regions: (i) pretransformation region, 930–1100 °C and (ii) coexistence region, 1100–1220 °C, in which characteristic reflexions of both phases are present in the diffraction pattern.

(a) Pretransformation

X-ray diffraction intensities are observed to decrease as usual in accordance with the Debye–Waller factor between room temperature and 900 °C. But an anomalous increase in the intensities of $11\bar{1}_m$ and 111_m is observed with increasing temperature in the pretransformation and is given in Table 1 and Fig. 1. In order to make sure that this anomalous increase is not due to factors like orientation effects, grain growth and mis-

Table 2. *Interplanar distances of some reflexions in the transition region on heating*

Temperature	$11\bar{1}_m$	111_m	101_t	002_m	020_m	200_m 110_t	002_t
1028 °C	3·152	2·854	—	2·643	2·586	2·549	
1069	3·157	2·857	—	2·647	2·589	2·552	
1110	3·155	2·856	—	2·648	2·589	2·550	
1130	3·155	2·852	—	2·647	2·587	2·552	
1151	3·151	—	2·973	2·647	2·586	2·550	
1159	3·152	—	2·973	2·647		—	
1167	3·156	2·852	2·968	2·645		2·555	2·617
1175	3·152	2·852	2·966			2·549	—
1186	3·152	2·852	2·964			2·549	2·613
1196	3·147	2·849	2·960			2·547	2·609
1206	3·157		2·957			—	—
1213			2·960			2·551	2·613

Table 3. *Intensities of some reflexions in the coexistence region (in arbitrary units)*

On heating								On cooling			
Temperature	$11\bar{1}_m$	101_t	111_m	002_m	020_m	200_m 110_t	002_t	Temperature	$11\bar{1}_m$	101_t	111_m
1028 °C	98	5	93	87·2	86·2	63		1314 °C		99·9	
1069	98	6	98	90	93·9	65		1237		100	
1110	100	7·9	100	97	100	72		1152		94·8	
								1026	6		
1130	99·3	13·8	95	100	93·9	72		1017	17·5		88
1151	87·8	24	—	95·9	89·3	76·1		1010	62		—
1159	76	35	—	—				1003	68	49	73·6
1167	55·0	61	44·6	54·9	82·2	98		993	71·6	47·2	78
1175	45·7	72·4	33·2	—	—			976	78·7	45·9	80·4
1186	34	80·5	27·0	26		100	88	958	81·2	35·7	82·4
1196	21·0	89·1	12·5			98	91	943	88	33·0	88
								921	89	30	92·2
1206	10	92·4	8					899	96·5	26	98
1213	6	96	6			98	94·8	872	98	22·6	98
1228	4	100				100	100	845	99	19	100
1309						92·5	88	799	100	15	100
1393						85·8	78	774	—	13·1	—
								748	—	13	—
								710	—	11·4	—

alignment, a number of experiments on different specimens and a set of two consecutive experiments on the same specimen were carried out. Although the data are not quantitatively reproducible, the anomalous increase in intensities is always found, prominently for $11\bar{1}_m$ and 111_m and slightly in case of 002_m, 020_m and 200_m. This excludes the possibility of orientation effects as it would require increase in intensity of some reflexions accompanied by a decrease in intensity of others. The factor of grain growth is also excluded because besides the evidence of substantial increase in intensities in a set of consecutive experiments (Table 1), there are anomalous changes in d values with temperature in the pretransformation region (Fig. 2 and Table 2). Misalignment of the surface of a sample after cycling was found to be less than 0·05° in 2θ, as has already been discussed (Patil & Subbarao, 1969). Referring to Fig. 4 it can be seen that $11\bar{1}_m$ and 111_m derive their intensities primarily from Zr atoms and receive relatively smaller contribution from oxygen atoms, but 002_m, 020_m and 200_m depend mostly on oxygen atoms for their intensities. Thus the anomalous increase in intensities, prominently for $11\bar{1}_m$ and 111_m and slightly in case of 002_m, 020_m and 200_m, is interpreted as a result of Zr atoms coming more and more in phase after changes in their positional parameters because of their vibrational excitation due to special modes. The anomalous expansion of selected d values in this temperature range (Fig. 2 and Table 2. See also Patil & Subbarao, 1969) serves as an additional support for the existence of special vibrational modes in this region. It may be mentioned here that Ubbelohde (1966) had recognized the existence of special vibrational modes in the premonitory phenomena observed in specific heat anomalies and that Cochran (1960) and Anderson (1960) had considered the temperature dependence of the frequency of the transverse optical modes in the ferroelectric transitions. It is also interesting to note at this point that even in dynamic differential thermal analysis studies with sufficiently low heating rates of the order of 1 °C.min⁻¹, the heat effect associated with the pretransformation behaviour could be clearly seen from the curves given by Ruh & Garrett (1968).

(b) Coexistence and hybrid crystal formation

The beginning of the coexistence region is signalled by the sharpening of 101_t at about 1100°C [Fig. 3(a)]. The intensity of 101_t increases with temperature at the expense of the corresponding monoclinic lines, viz. $11\bar{1}_m$ and 111_m, until $11\bar{1}_m$ and 111_m finally disappear at about 1220°C [Fig. 3(b)]. However, other lines characteristic of the tetragonal phase do not appear until about 1160°C [Fig. 3(c)]. In the region of 1160–1190°C following changes are noted. The reflexions 200_m and 020_m disappear when 110_t and 002_t appear at about 1160°C. However, 002_m persists and its intensity reduces considerably with increasing temperature beyond 1160°C until it finally disappears at 1190°C.

Also the interdependent changes in intensities of $11\bar{1}_m$, 111_m and 101_t undergo an inflexion point with respect to temperature dependence of their intensities in this region (Table 3 and Fig. 3). In this temperature region all these changes indicate that the atomic rearrangements along the a_m and b_m axes precede those along the c_m axis and appear to be mostly responsible in
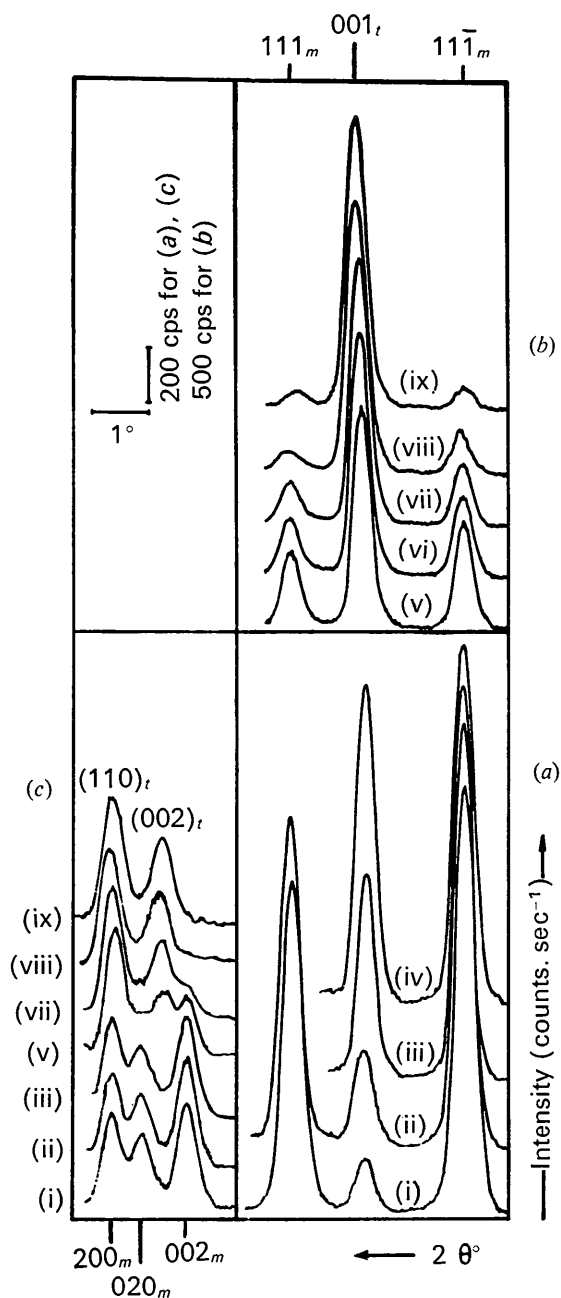

Fig. 3. X-ray diffraction maxima in the coexistence region of the monoclinic–tetragonal phase transition in ZrO_2 on heating. Corresponding crystallographic planes are indicated in the Figure. Records (i) to (ix) refer to temperature 1110, 1130, 1151, 1159, 1167, 1175, 1186, 1196, 1206°C respectively.

giving rise to 110_t and 002_t. Also it is seen that the a_m value is very near to $a_t\sqrt{2}$ (Fig. 2).
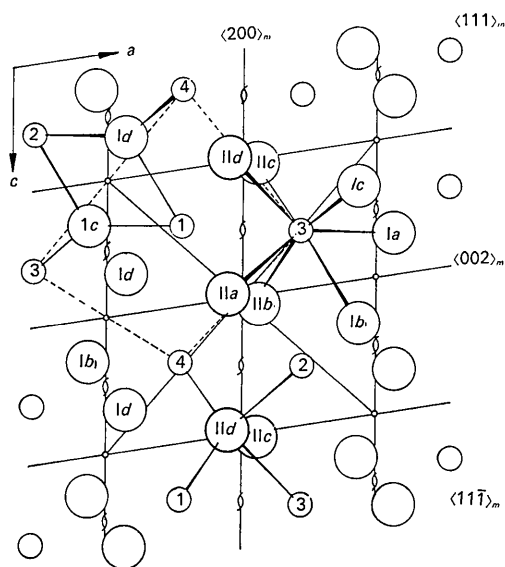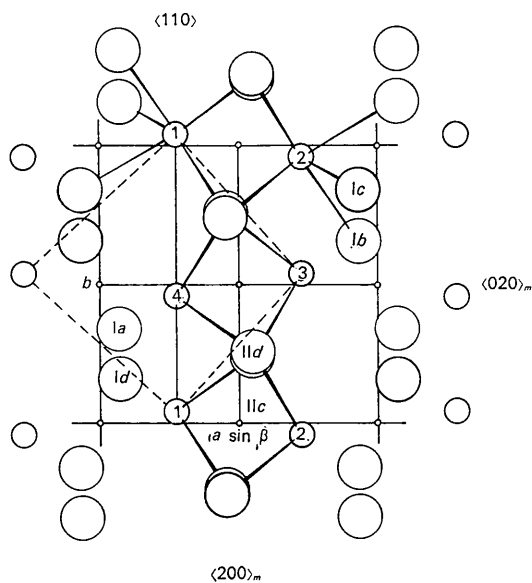

Fig. 4. Projection of the crystal structure of monoclinic ZrO_2 along the b_m axis (from McCullough & Trueblood, 1959). Broken lines show the projection of a pseudo-cell related to the tetragonal cell in the monoclinic structure if $[001]_t \parallel [010]_m$. $\langle 200 \rangle_m$, $\langle 111 \rangle_m$, $\langle 002 \rangle_m$ and $\langle 11\bar{1} \rangle_m$ indicate the lines of intersection of respectively $(200)_m$, $(111)_m$, $(002)_m$ and $(11\bar{1})_m$ with the plane of projection, $a_m - c_m$.

Fig. 5. Projection of the crystal structure of monoclinic ZrO_2 along the c_m axis (from McCullough & Trueblood, 1959). Broken lines show the projection of a pseudo-cell related to the tetragonal cell in the monoclinic structure if $[001]_t \parallel [001]_m$. $\langle 110 \rangle_t$, $\langle 002 \rangle_m$ and $\langle 200 \rangle_m$ indicate the lines of intersection of $(110)_t$, $(002)_m$ and $(200)_m$ respectively, with the plane of projection $a_m - b_m$.

In the coexistence region, either both of the distinct phases – monoclinic and tetragonal – of ZrO_2 are concurrently present or else a hybrid crystal structure is formed. It is more appropriate to think of hybrid crystal formation in the coexistence region rather than phase separation for the following reasons: (i) Only one reflexion, the 101_t, characteristic of the tetragonal form appears at $1110\,°C$, while other lines appear at $1160\,°C$ or above. Similarly, even after the disappearance of the high index monoclinic lines at about $1190\,°C$, $11\bar{1}_m$ and 111_m persist up to $1220\,°C$ (Fig. 3). (ii) Furthermore, with increasing temperature in the coexistence region, many interplanar spacings of the tetragonal form show a contraction instead of the usual thermal expansion to be expected in the case of a distinct phase (Fig. 3). Other important characteristics of this hybrid crystal are: (i) All reflexions present in the diffraction pattern can be indexed on either monoclinic or tetragonal structures and neither extra lines, if any, characteristic of this hybrid crystal structure nor any superstructure lines have been observed (ii) $11\bar{1}_m$, 111_m and 101_t show interdependence in their temperature dependent intensities in the coexistence region. Although, these observations seem to favour the view of possible hybrid crystal formation as a unique, ill-defined structure rather than that through coexisting domains, single-crystal data are necessary to shed further light on this problem. It should be mentioned here that hybrid crystal formation through coexisting domains during transitions in general has been discussed by Parry (1962); Parry, Schuyff & Ubbelohde (1965) and by Ubbelohde (1966).

(c) Orientation relationship

Many workers (Bailey, 1964; Grain & Garvie, 1965; McCullough & Trueblood, 1959; Wolten, 1964) have observed twinning on $(100)_m$ and the orientation relationship for planes,

$$(100)_m \parallel (110)_t,$$

is established. By selecting in the monoclinic structure, a pseudo-cell approximating either a face centred (Bailey, 1964) or a body centred tetragonal cell (Grain & Garvie, 1965), the following relationships of directions was indicated:

$$[001]_m \parallel [001]_t$$

However, Wolten's observations on a single crystal are not in agreement with the second relation and obviously demand due consideration. A pseudo-cell approximating a body centred tetragonal cell (Teufer, 1962) can be selected in the monoclinic structure in two ways if the first relation is considered to be established. c_t can either be along c_m or along b_m. Projections of these two cells are shown in Figs. 4 and 5 with dashed lines. In the coexistence region $a_m \geq a_t\sqrt{2}$ and $c_m > c_t > b_m > a_m$ (Patil & Subbarao, 1969) and the transition is accompanied by 3% volume contraction. Thus, if one takes c_t to be along c_m, there has to be contraction in all the

three directions during the transformation. However, in the second case there will be contraction in a_m and c_m values and expansion along b_m.

The following observations support the correlation in which the c_t axis is along b_m: (i) Wolten cycled the heat treatment of a single crystal through the transformation and observed a number of slightly misoriented blocks, still parallel along the original b_m direction but rotated out of register in the $a_m - c_m$ plane. (ii) In the region 1160–1190°C the atomic rearrangements along a_m and b_m axes precede those along c_m and appear to be mostly responsible for the appearance of 002_t and 110_t. Thus, giving weight to Wolten's single-crystal work and the present experimental evidence, the orientation relationship can be written as:

$$(100)_m \,||\, (110)_t \text{ plane}$$

$$[010]_m \,||\, [001]_t \text{ direction}$$

(d) Mechanism

In the monoclinic structure there are alternating layers of $O_{II}Zr_4$ distorted tetrahedra and approximately triangular O_IZr_3 coordination polyhedra, which share Zr atoms. These Zr atoms form layers, parallel to $(100)_m$, with two different interlayer distances as shown in Fig. 6. The Zr atoms on any one of these layers have O_{II} atoms on one side and O_I atoms on the other side of the layer. The distance between two layers of Zr atoms is larger when these layers are separated by O_I atoms than when they are separated by O_{II} atoms. It is obvious that these interlayer distances become equal in the tetragonal phase through the movement of O_I atoms. The O_I atoms would have to attain the tetrahedral surrounding during the transformation. It becomes clear from the geometry of the monoclinic structure that when any O_I atom (such atom is marked I' in Fig. 6) is surrounded by a triangular arrangement of three Zr atoms, the choice of the fourth Zr atom is limited to a specific Zr atom in the neighbourhood, marked as 1' in Fig. 6. This Zr atom is positioned on the line passing through the O_I atom and very nearly perpendicular to the plane of the three Zr neighbours (broken arrow line in Fig. 6). The directions of the possible atomic movements of the O_I atoms resulting from the above working principle (broken arrow line) agree closely with the intuitive suggestions of Smith & Newkirk, 1965 (continuous arrow line) as seen from Fig. 7. This is also in agreement with the mechanism given by Grain & Garvie for the transformation. It may be mentioned that while the directions of atomic movements are established, their magnitude could not be determined.

The changes in the temperature range 1160–1190°C can be interpreted best by focusing attention on the central Zr atom and its near neighbours in the pseudo-cell as shown in Fig. 4 (see Fig. 8 of the tetragonal cell for comparison). In monoclinic ZrO_2, the Zr atom is surrounded by seven oxygen atoms. Four of them termed $O_{II}^{(m)}$, are at 2·189, 2·220, 2·151, 2·285 Å and

three, termed $O_T^{(m)}$, at 2·057, 2·163, 2·051 Å. This complex irregular arrangement changes over to the high temperature tetragonal form, in which each Zr atom is surrounded by eight oxygen atoms, four of them ($O_{II}^{(t)}$) at 2·455 Å and the other four ($O_T^{(t)}$) at 2·065 Å. From Fig. 4 and the orientation relationship [3.1(c)], it becomes clear that $O_{II}^{(m)}$ atoms move in the
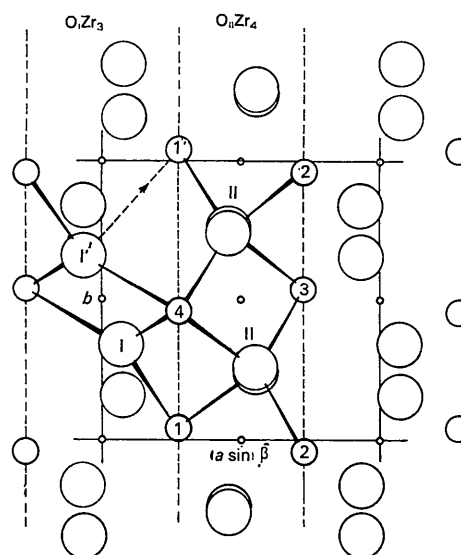

Fig. 6. Projection of the crystal structure of monoclinic ZrO_2 along the c_m axis showing layers of O_IZr_3 and $O_{II}Zr_4$ polyhedra (after McCullough & Trueblood, 1959). The Zr atom marked 1' is unique in the neighbourhood of O_I atom which is marked 1'.
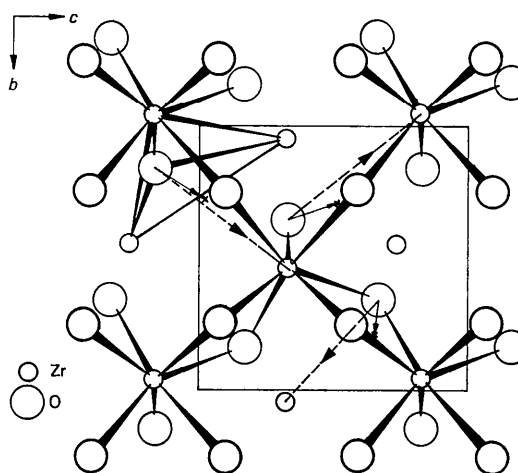

Fig. 7. The layer of ZrO_7 groups at $x=\frac{1}{4}$ projected on the $(100)_m$ plane. The unit-cell outline represents its position at $x=0$. The small crosses show the oxygen positions in the tetragonal form (after Smith & Newkirk, 1965). One O_IZr_3 polyhedron is shown in bold. The small continuous arrows indicate the probable movement of oxygen at the phase change according to Smith & Newkirk, while dotted arrow lines show the directions of probable atomic movements as discussed in the text.

$(200)_m$ plane in the region 1160–1190°C, mostly in the direction of the b_m axis and thereby two of them come nearer to the central Zr atom while the other two go farther from it. That is to say, two of them become $O_I^{(p)}$ and the other two $O_{II}^{(p)}$. In the $O_I^{(m)}$ polyhedron two $O_I^{(m)}$ atoms become $O_I^{(p)}$ and the third $O_I^{(m)}$ atom becomes $O_{II}^{(p)}$. However, it should be mentioned that in the above temperature region not only $O^{(m)}$ atoms but also other atoms, Zr and $O_{II}^{(m)}$, undergo substantial movements. All these changes result in eightfold coordination for Zr and fourfold coordination for all oxygen atoms.

Tetragonal–monoclinic transition

The onset of the tetragonal–monoclinic transition is quite different from that of the monoclinic–tetragonal transition. The coexistence region in the monoclinic–tetragonal transition is preceded by a pretransformation region and its beginning is signalled by clear appearance of 101_t which does not appear concurrently with other reflexions of the tetragonal phase, while in the tetragonal–monoclinic transition there is no evidence of a similar pretransformation region (Fig. 9). The concurrent and drastic changes in the narrow temperature range of ± 5°C around 1020°C

as seen from Fig. 9 are interpreted as a cooperative change in both short and long range interactions. In other words the tetragonal phase is unstable as a whole in this narrow temperature region and a drastic change is exhibited. Below the transition temperature only 101_t persists up to 700°C and the hybrid crystal of monoclinic-based type is an equilibrium structure in the region of transition temperature to 700°C if the test temperatures maintained for 5 to 10 minutes can be assumed to represent near equilibrium conditions. This is justified in view of the diffusionless nature of the transition and the fact that the transition cannot be quenched. The large extent of the coexistence region below the transition temperature can probably be explained if establishment of new short and long range order characteristic of the complex monoclinic structure is supposed to show slow temperature dependence.

The origin of the large thermal hysteresis

The range of the coexistence region during heating and cooling, as determined from the present study, are compared with earlier results in Table 4. The difference between the transition temperatures, designated by the inflexion points of the intensity versus temperature curves, was used to estimate the thermal hysteresis. It is about 160°C in the present study.
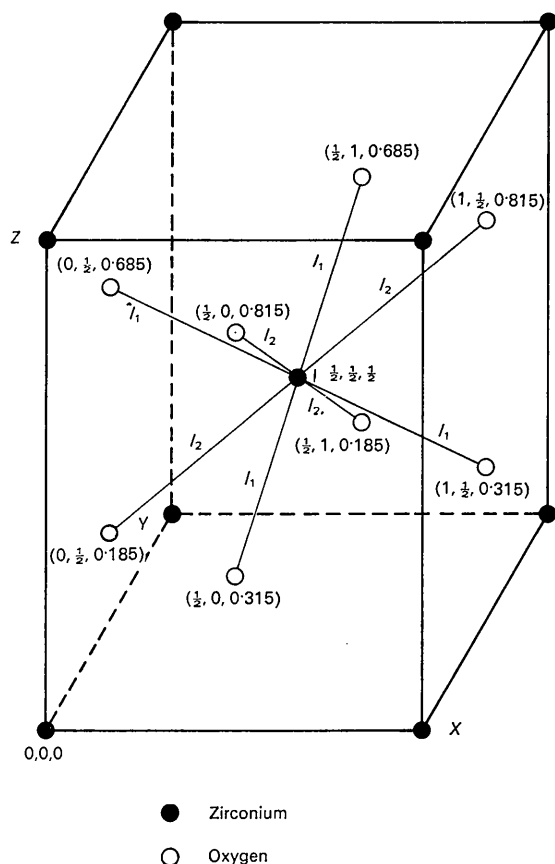
Table 4. Coexistence region from different sources

Source	Observed region	
	On heating	On cooling
Baun (1963)	1000–1200°C	970–750°C
Hinz & Dietzel (1962)	1150–1200	1000–700
Fehrenbacher & Jacobson (1965)	1130–1200	1025–950
Grain & Garvie (1965)	1130–1230	1000–550
Present study	1100–1220	1030–700

Ubbelohde (1966) has correlated the thermal hysteresis in transitions with the volume change and Lightstone (1967) related it to the characteristic defect structures in case of martensitic transitions. However, these types of correlations do not appear to help in gaining insight as to the origin of the thermal hysteresis.

The present study shows that there exist two distinctly different mechanisms for the transition in ZrO_2 in the two cases of heating and cooling. During heating the Zr atoms are vibrationally excitable and the pretransformation behaviour is observed. This gives rise to a considerable spread of the transformation before the transition temperature is approached during heating. On the other hand, during cooling the pretransformation behaviour is absent and there is a drastic change in a small temperature range near the transition temperature indicating the instability of the high temperature phase as a whole. This is interpreted as a cooperative change in both short and long range interactions. This distinct difference in mechanisms of the transition, one locally started during heating and the other cooperatively started during cooling, is

● Zirconium

○ Oxygen

Fig. 8. The tetragonal unit cell (Teufer, 1962). $l_1 = $Zr–$O_I = $ 2·065 Å and $l_2 = $Zr–$O_{II} = $2·455 Å.

plausibly suggested to be origin of the large thermal hysteresis in the transition in ZrO_2.

Conclusions

The pretransformation region distinct from the co-existence region in the monoclinic–tetragonal transition in ZrO_2 has been identified. Changes in the positional parameters of Zr atoms due to their vibrational excitation seem to be responsible for the anomalous intensity changes in the pretransformation region. This, followed by the behaviour in the coexistence region discussed in terms of the sequence of changes and atomic movements, forms a convincing picture of the mechanism for the monoclinic–tetragonal transition. The orientation relationship between the two structures is now established as follows:

$$(100)_m \,||\, (110)_t$$
$$[010]_m \,||\, [001]_t$$

A closer look at the coexistence region in the monoclinic–tetragonal as well as tetragonal–monoclinic transition revealed the validity of the concept of hybrid crystal formation in the coexistence region. It is seen that the mechanism of the tetragonal–monoclinic transition differs noticeably from that of the monoclinic–tetragonal transition, which is suggested to be the origin of the large thermal hysteresis.

The authors are grateful to U.S. National Bureau of Standards for financial support and to Dr C. N. R. Rao, Dr D. Chakravorty and Dr D. K. Smith for their helpful comments.

References

ANDERSON, P. W. (1960). *Fizika Dielektrikov, Izd. Akad. Nauk SSR, Moscow.* Paper presented at All-Union Conference Dielectrics, Moscow, 1958.

BAILEY, J. (1964). *Proc. Roy. Soc.* A**279**, 395.

BAUN, W. L. (1963). *Science,* **140**, 1330.

COCHRAN, W. (1960). *Advanc. Physics,* **9**, 387.

CYPRES, R., WOLLAST, R. & RAUEQ, J. (1963). *Ber. dtsch. keram. Ges.* **40**, 527.

FEHRENBACHER, L. L. & JACOBSON, L. A. (1965). *J. Amer. Ceram. Soc.* **48**, 157.

GAVRISH, A. M. & KRIVORUCHKO, P. P. (1966). 7th International Congress and Symposium, I. U. Cr. *Acta Cryst.* **21**, A195.

GRAIN, C. F. & GARVIE, R. C. (1965). U. S. Bur. Mines Report No. 6619.

HINZ, I. & DIETZEL, A. (1962). *Ber. dtsch. keram. Ges.* **39**, 489.

LIGHTSTONE, J. B. (1967). *Acta Metallurg.* **15**, 25.

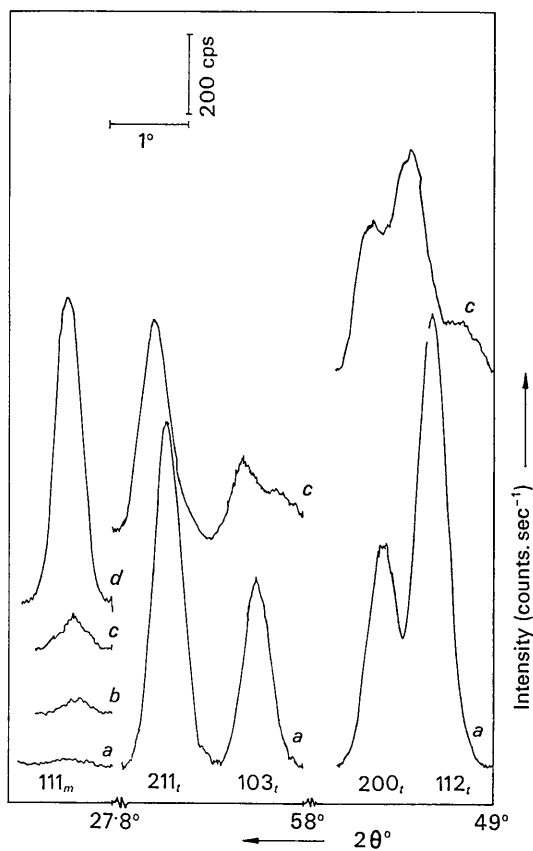McCULLOUGH, J. D. & TRUEBLOOD, K. N. (1959). *Acta Cryst.* **12**, 507.

Fig. 9. Reflexions showing sudden onset of the tetragonal–monoclinic phase transition in ZrO_2 while cooling, correspond to 112_t, 200_t, 103_t, 211_t and $11\bar{1}_m$. Records a, b, c and d refer to temperatures 1152, 1026, 1016 and 1010°C respectively.

PARRY, G. S. (1962). *Acta Cryst.* **15**, 596, 601.

PARRY, G. S., SCHUYFF, A. & UBBELOHDE, A. R. (1965). *Proc. Roy. Soc.* A**285**, 360.

PATIL, R. N. & SUBBARAO, E. C. (1969). *J. Appl. Cryst.* **2**, 281.

RUH, R. & GARRETT, M. J. (1968). 2nd International Conference on Thermal Analysis (To be published in *Thermal Analysis*).

SMITH, D. K. & NEWKIRK, H. W. (1965). *Acta Cryst.* **18**, 983.

SUKHAREVSKII, B. YA., ALAPIN, B. G. & GAVRISH, A. M. (1964). *Doklady Akad. Nauk SSSR,* **156**, 677.

TEUFER, G. (1962). *Acta Cryst.* **15**, 1187.

UBBELOHDE, A. R. (1956). *Quart. Rev. Chem. Soc.* **11**, 246.

UBBELOHDE, A. R. (1966). *J. Chim. Phys.* **1**, 33.

WHITNEY, E. D. (1962). *J. Amer. Ceram. Soc.* **45**, 612.

WOLTEN, G. M. (1963). *J. Amer. Ceram. Soc.* **46**, 418.

WOLTEN, G. M. (1964). *Acta Cryst.* **17**, 763.